RadioGraphics

Pulmonary Sarcoidosis: Typical and Atypical Manifestations at High-Resolution CT with Pathologic Correlation[1]

Eva Criado, MD • Marcelo Sánchez, MD • José Ramírez, MD, PhD • Pedro Arguis, MD • Teresa M. de Caralt, MD, PhD • Rosario J. Perea, MD, PhD • Antonio Xaubet, MD, PhD

CME FEATURE

See www.rsna.org/education/rg_cme.html

LEARNING OBJECTIVES FOR TEST 3

After reading this article and taking the test, the reader will be able to:

- Describe the differential diagnosis of pulmonary sarcoidosis.
- Discuss the role of high-resolution CT in the diagnosis and management of pulmonary sarcoidosis.
- Recognize typical and atypical features of pulmonary sarcoidosis at high-resolution CT.

TEACHING POINTS

See last page

Sarcoidosis is a multisystem disorder that is characterized by noncaseous epithelioid cell granulomas, which may affect almost any organ. Thoracic involvement is common and accounts for most of the morbidity and mortality associated with the disease. Thoracic radiologic abnormalities are seen at some stage in approximately 90% of patients with sarcoidosis, and an estimated 20% develop chronic lung disease leading to pulmonary fibrosis. Although chest radiography is often the first diagnostic imaging study in patients with pulmonary involvement, computed tomography (CT) is more sensitive for the detection of adenopathy and subtle parenchymal disease. Pulmonary sarcoidosis may manifest with various radiologic patterns: Bilateral hilar lymph node enlargement is the most common finding, followed by interstitial lung disease. At high-resolution CT, the most typical findings of pulmonary involvement are micronodules with a perilymphatic distribution, fibrotic changes, and bilateral perihilar opacities. Atypical manifestations, such as masslike or alveolar opacities, honeycomb-like cysts, miliary opacities, mosaic attenuation, tracheobronchial involvement, and pleural disease, and complications such as aspergillomas, also may be seen. To achieve a timely diagnosis and help reduce associated morbidity and mortality, it is essential to recognize both the typical and the atypical radiologic manifestations of the disease, take note of features that may be suggestive of diseases other than sarcoidosis, and correlate imaging features with pathologic findings to help narrow the differential diagnosis.

Abbreviation: HE = hematoxylin-eosin

RadioGraphics 2010; 30:1567–1586 • **Published online** 10.1148/rg.306105512 • **Content Codes:** CH CT

[1]From the Departments of Radiology (E.C., M.S., P.A., T.M.d.C., R.J.P.), Pathology (J.R.), and Pneumology (A.X.), Hospital Clínic de Barcelona, C/ Villarroel 170, 08036 Barcelona, Spain. Presented as an education exhibit at the 2009 RSNA Annual Meeting. Received February 5, 2010; revision requested March 23 and final revision received May 25; accepted June 9. For this CME activity, the authors, editors, and reviewers have no relevant relationships to disclose. **Address correspondence to** E.C. (e-mail: *eva-criado@hotmail.com*).

Teaching Point

RadioGraphics

Introduction

Sarcoidosis is a multisystem chronic inflammatory condition of unknown etiology. It is characterized by noncaseous epithelioid cell granulomas and changes in tissue architecture, which may affect almost any organ. Involvement of the lung and the mediastinal and hilar lymph nodes is most common, being seen in approximately 90% of patients, and accounts for most of the morbidity and mortality associated with the condition (1).

The article focuses on the thoracic manifestations of sarcoidosis and explores the role of high-resolution computed tomography (CT), in particular, for its diagnosis and management. Typical and atypical radiologic appearances are described (Table 1) and correlated with pathologic findings.

Epidemiology

The incidence of sarcoidosis varies widely throughout the world, probably because of differences in environmental exposure, surveillance methods, and predisposing genetic factors. Demographic factors, including race, ethnicity, age, and sex, markedly affect local incidence. There is also scientific evidence of familial clustering of sarcoidosis (2).

Although sarcoidosis can affect patients of any age, sex, or race, it typically affects adults less than 40 years old, and the incidence peaks in the 3rd decade of life (ages 20–29 years). In most studies, a slightly higher rate of occurrence has been found among women than among men, across racial and ethnic groups (3).

Estimates of the prevalence of sarcoidosis range from less than one case to 40 cases per 100,000 people in the general population. In the United States, the age-adjusted annual incidence among blacks is more than triple that among whites (35.5 vs 10.9 per 100,000 inhabitants) (4). Black Americans, Swedes, and Danes appear to have the highest prevalence worldwide (5). Sarcoidosis is rarely reported in India, Saudi Arabia, Spain, Portugal, and South America, perhaps partly because of the absence of mass screening programs and partly because granulomatous pulmonary disease is attributed to other, more common causes, such as tuberculosis, leprosy, and fungal infections (1,5,6).

The manifestations and natural history of sarcoidosis are also influenced by epidemiologic factors. Whites often present without symptoms, whereas blacks often present with severe multisystem disease (1,7). Higher mortality rates have been reported in the black population; however, these data may be somewhat biased because of differences in access to health care (8).

Clinical Features

The most common clinical features at presentation are respiratory symptoms (eg, cough, dyspnea, bronchial hyperreactivity), fatigue, night sweats, weight loss, and erythema nodosum. However, as many as 50% of cases of sarcoidosis are asymptomatic, with abnormalities detected incidentally at chest radiography (9,10).

Pulmonary function tests typically demonstrate a restrictive ventilatory defect with decreased volumes and decreased carbon monoxide diffusing capacity. These functional alterations tend to become more frequent and marked from stage 1 to stage 4 (11). If endobronchial sarcoidosis is present, an obstructive ventilatory defect may occur. Airway obstruction is found in 5.7% of cases of pulmonary involvement in sarcoidosis (12); it is associated with increased morbidity, greater frequency of respiratory symptoms, and radiographic stage 4 disease, and it is therefore considered an indicator of a poor prognosis (13).

The clinical course varies (14). Nearly two-thirds of patients with sarcoidosis generally remain stable or experience a remission within a decade after diagnosis, with few or no consequences thereafter. However, approximately 20% of patients develop chronic disease leading to pulmonary fibrosis (1,15). Recurrence after a remission lasting 1 year or more is uncommon (<5% of patients), but recurrent disease may develop at any age and in any organ. Less than 5% of patients die of sarcoidosis; death from sarcoidosis is usually the result of extensive and irreversible lung fibrosis with respiratory failure or cardiac or neurologic involvement (1,9,16).

Factors associated with a poor prognosis include stage 2 or 3 pulmonary disease at the time of initial diagnosis, disease onset after the age of 40 years, black race (7), hypercalcemia (14), splenomegaly, osseous involvement (14), chronic uveitis (14), and lupus pernio (9). Common early-stage features that are associated with a good prognosis (spontaneous remission rate of >85%) are fever, polyarthritis, erythema nodosum, and bilateral hilar lymph node enlargement (Löfgren syndrome) (9).

Pathogenesis

Sarcoidosis is an immune-mediated multisystem disease. The most widely accepted explanation of the pathogenesis of sarcoidosis is that one or more specific environmental agents trigger an inflammatory response in the immune system

Table 1
Typical and Atypical Features of Pulmonary Sarcoidosis at High-Resolution CT

Typical features
Lymphadenopathy: hilar, mediastinal (right paratracheal), bilateral, symmetric, and well defined
Nodules: micronodules (2–4 mm in diameter; well defined, bilateral); macronodules (≥5 mm in diameter, coalescing)
Lymphangitic spread: peribronchovascular, subpleural, interlobular septal
Fibrotic changes: reticular opacities, architectural distortion, traction bronchiectasis, bronchiolectasis, volume loss
Bilateral perihilar opacities
Predominant upper- and middle-zone locations of parenchymal abnormalities
Atypical features
Lymphadenopathy: unilateral, isolated, anterior and posterior mediastinal
Airspace consolidation: masslike opacities, conglomerate masses, solitary pulmonary nodules, confluent alveolar opacities (alveolar sarcoid pattern)
Ground-glass opacities
Linear opacities: interlobular septal thickening, intralobular linear opacities
Fibrocystic changes: cysts, bullae, blebs, emphysema, honeycomb-like opacities with upper- and middle-zone predominance
Miliary opacities
Airway involvement: mosaic attenuation pattern, tracheobronchial abnormalities, atelectasis
Pleural disease: effusion, chylothorax, hemothorax, pneumothorax, pleural thickening, calcification
Pleural plaquelike opacities
Mycetoma, aspergilloma

of a genetically susceptible host. However, the supposed antigenic agents responsible for the disease have yet to be identified (17). Epithelioid cell granulomas are a result of stimulation of cell-mediated immunity. Activated alveolar macrophages and T cells release interleukin-1, fibronectin, and alveolar macrophage-derived growth factor, which in turn activate and recruit additional T cells and fibroblasts. The population of activated T cells releases other factors (interleukin-2, monocyte chemotactic factor, and immune interferon), which stimulate and recruit additional immune cells. The process may resolve spontaneously, or it may progress to the extensive formation of noncaseous granulomas (the characteristic histologic feature of sarcoidosis) and fibrosis (17).

Histologic Findings

The histologic hallmark of sarcoidosis is noncaseous granulomas composed of a central core of histiocytes, epithelioid cells, and multinucleated giant cells surrounded by lymphocytes, scattered plasma cells, and varying quantities of fibroblasts and collagen in the periphery (18). The giant cells may contain cytoplasmic inclusions such as asteroid bodies and Schaumann bodies. The central portion of the granuloma consists predominantly of lymphocytes that express CD4 protein, whereas lymphocytes that express CD8 are found in the peripheral zone. Dense bands of fibroblasts, mast cells, collagen, and proteoglycans may encase the granuloma and lead to fibrosis, end-organ damage, and irreversible disruption of organ function (19). Fibrotic changes usually begin at the periphery of a granuloma and extend centrally, leading to complete fibrosis, hyalinization, or both. Granulomas occasionally exhibit focal coagulative necrosis (19), and it has been suggested that necrotizing sarcoid granulomatosis may be a variant of sarcoidosis (20).

Teaching Point

Granulomas in the lung parenchyma have a characteristic distribution in relation to lymphatics in the peribronchovascular interstitial space, subpleural interstitial space, and, to a lesser extent, the interlobular septa (ie, a lymphangitic distribution). The upper lobes of the lungs are most severely affected. Vascular involvement is observed in more than half of patients with sarcoidosis who undergo an open lung biopsy or autopsy study (21).

Staging and Prognosis

Teaching Point

More than 40 years ago, Siltzbach developed a sarcoidosis staging system based on the pattern of chest radiographic findings, a system still widely used because of its great prognostic value (22).

Staging of Sarcoidosis on the Basis of Chest Radiographs

STAGE 0	No abnormalities	5%–10%
STAGE 1	Lymphadenopathy (fig. A)	50%
STAGE 2	Lymphadenopathy + pulmonary infiltration (fig. B)	25%–30%
STAGE 3	Pulmonary infiltration (fig. C)	10%–12%
STAGE 4	Fibrosis	5% (up to 25% during the course of the disease)

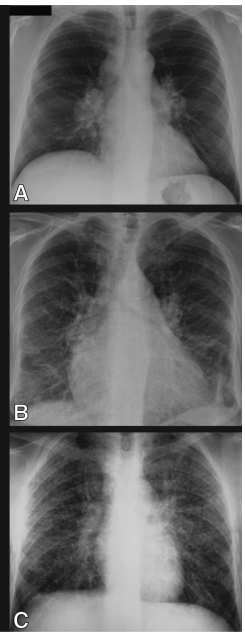

Figure 1. Chart shows the system for staging of sarcoidosis on the basis of chest radiographic findings. Percentages indicate the proportion of the population with a diagnosis of sarcoidosis who had the stage of disease at presentation.

The Siltzbach classification system defines the following five stages of sarcoidosis: stage 0, with a normal appearance at chest radiography; stage 1, with lymphadenopathy only; stage 2, with lymphadenopathy and parenchymal lung disease; stage 3, with parenchymal lung disease only; and stage 4, with pulmonary fibrosis (3) (Fig 1).

At presentation, approximately 5%–10% of patients have stage 0 disease; 50%, stage 1; 25%–30%, stage 2; and 10%–12%, stage 3 (7). Although in most patients the condition either regresses or remains stable, it progresses to pulmonary fibrosis in approximately one-fourth of patients. Generally, pulmonary function worsens with more advanced disease stages, but the radiographic stage does not correlate well with the severity of pulmonary function abnormalities.

Spontaneous remission occurs in 60%–90% of patients with stage 1 disease, in 40%–70% with stage 2 disease, in 10%–20% with stage 3 disease, and in 0% with stage 4 disease (3,7).

This radiographic staging scheme was developed before the introduction of CT, and the data collected with regard to prognosis are based on findings at chest radiography, not CT. CT, especially high-resolution CT, is far more sensitive than chest radiography in depicting subtle parenchymal abnormalities in early stages of the disease, even in stage 1, which is associated with an excellent long-term prognosis (1,9); nevertheless, the prognostic value of CT findings has not yet been extensively studied (16).

Diagnosis

A diagnosis of sarcoidosis is established on the basis of compatible clinical and radiologic findings and histologic evidence of the presence of noncaseous epithelioid cell granulomas in one or more organs and the absence of causative organisms or particulates (16). Granulomas of known causes and local sarcoidlike reactions must be excluded. Granulomatous lesions may result from many conditions, including tuberculosis, berylliosis, leprosy, hypersensitivity pneumonitis, Crohn disease, primary biliary cirrhosis, and fungal disease. Moreover, local sarcoidlike reactions may be seen in lymph nodes that drain a neoplasm or a site of chronic inflammation (19). Such reactions also have been seen in patients who have undergone chemotherapy and radiation therapy (23).

If biopsy of lymph nodes or pulmonary or pleural tissue is necessary for diagnosis, one of three techniques may be used: transbronchial biopsy, CT-guided biopsy, or surgical biopsy (24). The use of a surgical technique may be warranted when the results of biopsy with another procedure are not definitive and biopsy of mediastinal lymph nodes, lung, or both is required. This can generally be done with minimally invasive procedures, such as cervical mediastinoscopy, the Chamberlain procedure (a parasternal minithoracotomy for biopsy of the aortopulmonary window or para-aortic nodes), or video-assisted thoracoscopic surgical biopsy (25).

The development of endobronchial ultrasonography (US) is one of the most important recent advances in bronchial imaging. Endobronchial US combined with fine-needle aspiration biopsy is a

Table 2
Reversible and Irreversible Abnormalities of Pulmonary Sarcoidosis at High-Resolution CT

Reversible parenchymal abnormalities*
Micronodules, macronodules
Airspace consolidation: confluent alveolar opacities
Ground-glass opacities
Interlobular septal thickening
Intralobular linear opacities
Irreversible parenchymal abnormalities†
Honeycomb-like opacities, cysts, bullae, emphysema
Architectural distortion
Traction bronchiectasis, bronchiolectasis
Volume loss in upper lobes, retraction of hila
Mycetoma (in 10% of patients with end-stage sarcoidosis and a preexisting cavity)

*These features are suggestive of granulomatous inflammation.
†These features are indicative of chronicity and fibrosis.

minimally invasive technique that is now routinely used in many pulmonary centers, where it may replace more invasive methods such as mediastinoscopy for evaluating enlarged mediastinal or hilar lymph nodes because it helps improve the diagnostic yield. Its clinical application and diagnostic benefit have been established in studies in which it was compared with conventional radiologic methods and other diagnostic procedures (26,27).

When the presence of pulmonary sarcoidosis is suspected, diagnostic procedures should ideally allow *(a)* histologic verification, *(b)* assessment of the extent and severity of organ involvement, *(c)* assessment of whether disease is stable or likely to progress, and *(d)* determination of whether a patient might benefit from treatment (1).

Use of High-Resolution CT

High-resolution CT has proved superior to conventional CT for assessing subtle parenchymal details and discriminating between inflammation and fibrosis in patients with pulmonary sarcoidosis (28–30). The thin-section collimation (1- to 1.5-mm section thickness) and high-spatial-frequency reconstruction algorithms that are used to generate high-resolution CT images allow improved detection of nodular and reticular opacities, thickened interlobular septa, and faint ground-glass opacities, making the technique especially useful for identifying and managing sarcoidosis.

Teaching Point

High-resolution CT may be particularly helpful for distinguishing active inflammation from irreversible fibrosis in selected patients with stage 2 or 3 sarcoidosis. Nodules, ground-glass opacities, and alveolar opacities are suggestive of granulomatous inflammation that may be reversed with therapy (31). By contrast, honeycomb-like cysts, bullae, broad and coarse septal bands, architectural distortion, volume loss, and traction bronchiectasis are indicative of irreversible fibrosis (16) (Table 2). High-resolution CT may be useful also for verifying specific diagnoses in patients with atypical clinical manifestations or unusual radiographic features (32).

In the appropriate clinical context, the observation of typical imaging features of sarcoidosis (eg, bilateral hilar lymph node enlargement with a perilymphatic micronodular pattern) and the anatomic distribution of those abnormalities (eg, upper lobe predominance) may point to a highly specific diagnosis. However, atypical manifestations may necessitate a broader differential diagnosis that includes tuberculosis and other granulomatous infections, silicosis, malignancies, and pneumoconiosis.

Radiologic-Pathologic Correlation

Open lung biopsies are rarely performed in patients with sarcoidosis. However, Nishimura et al (33) correlated histopathologic findings with CT features in eight patients with sarcoidosis in whom open lung biopsies had been performed. Thickened bronchovascular bundles and small perivascular nodules seen at CT corresponded to granulomas within the connective tissue sheath surrounding pulmonary airways and vessels. Pleural or subpleural nodules were correlated with granulomas adjacent to the visceral pleura. Ground-glass opacities represented an accumulation of many granulomatous lesions, with or without fibrosis, in the alveolar septa and around the small vessels. No alveolitis was seen. Large parenchymal nodules (>1 cm in diameter) represented coalescent granulomas. Air bronchiolograms within regions of dense consolidation on CT images corresponded to bronchiolar dilatation with surrounding fibrosis and a honeycomb-like pattern of microscopic cysts seen at pathologic analysis. In a series of 60 patients with sarcoidosis, CT findings of airway abnormalities (eg, bronchial wall thickening, bronchial luminal narrowing or stenosis) were correlated with bronchial granulomas in biopsy specimens (34).

Collections of granulomas form nodular features with a diameter of several millimeters or more (micronodules) on CT images. Coalescent groups of micronodules may form larger opacities

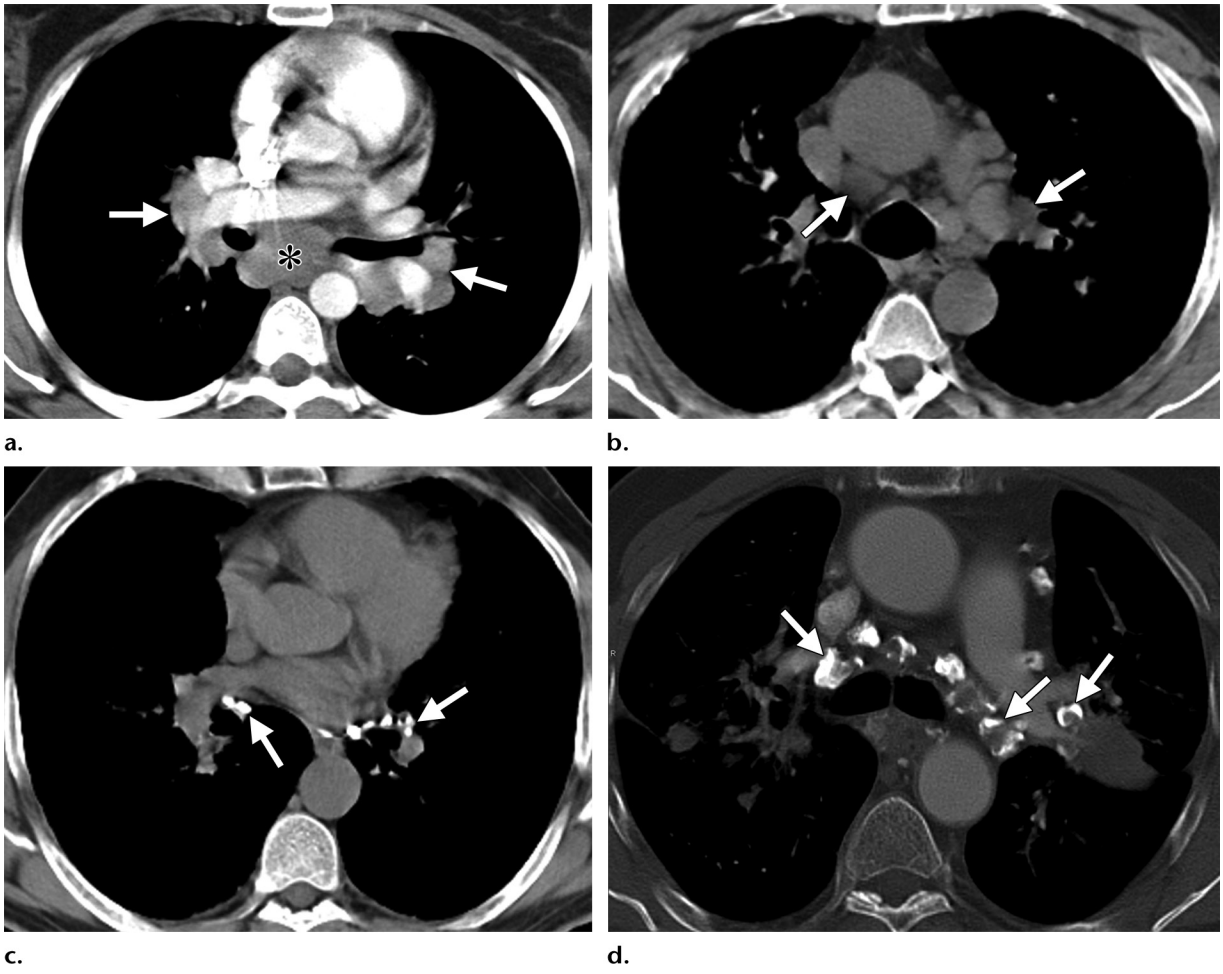

Figure 2. Typical **(a, b)** and atypical **(c, d)** radiologic findings of lymphadenopathy in four patients with sarcoidosis. **(a)** Axial contrast material–enhanced CT scan (mediastinal window) shows typical bilateral and symmetric hilar (arrows) and subcarinal (*) lymphadenopathy. **(b)** Axial unenhanced CT scan (mediastinal window) obtained at the level of the left pulmonary artery shows enlargement of right paratracheal and left hilar lymph nodes (arrows). Although the right hilum is not shown, it too was affected. **(c)** Axial unenhanced CT scan (mediastinal window) shows punctate calcifications of hilar lymph nodes (arrows), a pattern that also occurs in other chronic granulomatous diseases. **(d)** Axial contrast-enhanced CT scan shows bilateral eggshell-like calcifications of hilar and mediastinal lymph nodes (arrows), findings that warrant the inclusion of silicosis in the differential diagnosis in this case.

and masses, mimicking alveolar consolidation with or without air bronchograms on chest radiographs and CT images.

Typical Patterns of Lymphadenopathy

Teaching Point

The most common pattern is well-defined, bilateral, symmetric hilar and right paratracheal lymph node enlargement. Bilateral hilar lymph node enlargement, alone or in combination with mediastinal lymph node enlargement, occurs in an estimated 95% of patients affected with sarcoidosis (4,8,9). Middle mediastinal nodes (at the left paratracheal level, subcarinal level, and level of the aortopulmonary window), prevascular nodes, or both are involved in approximately 50% of patients (28) (Figs 2a, 2b).

Bilateral hilar lymph node enlargement may be a feature of infection (particularly fungal or mycobacterial infection) or malignancy (eg, lymphoma). However, in the absence of specific symptoms or signs, sarcoidosis is the most common cause of bilateral lymph node enlargement. In a sentinel study of 100 patients in whom bilateral lymph node enlargement was seen at chest radiography, sarcoidosis was the final diagnosis in 74 cases (35). The authors concluded that the risk of malignancy is low in patients with bilateral lymph node enlargement and no history of malignancy, provided that findings at physical examination and routine

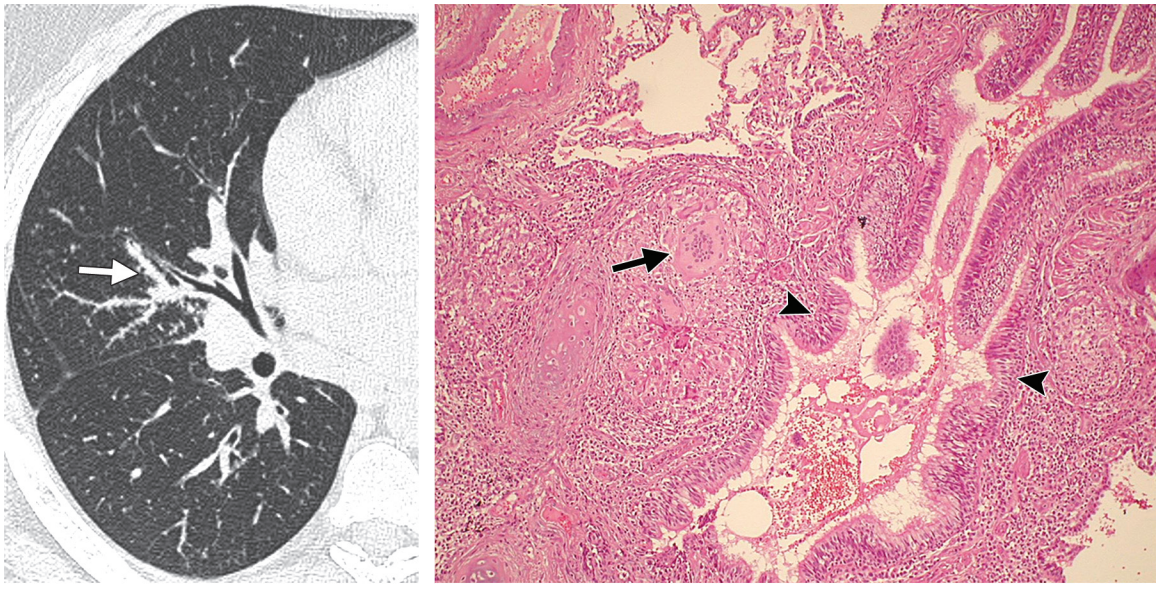

a. b.

Figure 3. **(a)** Axial high-resolution CT scan of the right lung in a woman with pulmonary sarcoidosis shows the typical perilymphatic distribution of micronodules (arrow). **(b)** Photomicrograph (original magnification, ×100; hematoxylin-eosin [H-E] stain) of a lung biopsy specimen demonstrates numerous epithelioid granulomas (arrow) surrounding the bronchial walls and immediately beneath the normal bronchial epithelium (arrowheads).

blood tests are normal. Histologic confirmation is not required for a diagnosis of sarcoidosis in these patients. However, a biopsy should be performed if the chest radiographic findings worsen or specific signs and symptoms develop.

Atypical Patterns of Lymphadenopathy

Occasionally, radiologic findings of lymph node enlargement may be asymmetric or seen in unusual locations (eg, internal mammary, paravertebral, and retrocrural regions). Such findings should lead to the inclusion of entities such as lymphoma or tuberculosis in the differential diagnosis. Isolated unilateral hilar lymph node enlargement (usually on the right side) is seen in less than 5% of cases. Enlargement of mediastinal lymph nodes without hilar lymph node enlargement is even less common (17,32,36,37).

The enlarged nodes eventually may become calcified. The occurrence of lymph node calcification in sarcoidosis, as in other chronic granulomatous diseases, is closely related to the duration of disease; calcification occurs in 3% of patients after 5 years and in 20% after 10 years (17). The calcifications may have an amorphous, punctate (Fig 2c), popcornlike, or eggshell-like appearance. Eggshell-like calcifications also may be seen in silicosis (36) (Fig 2d), and the other patterns of lymph node calcification in sarcoidosis may be indistinguishable from those seen in tuberculosis and histoplasmosis.

Atypical patterns of lymphadenopathy occur more frequently in patients older than 50 years (37).

Typical Parenchymal Manifestations

Micronodules with a Perilymphatic Distribution

A perilymphatic distribution of micronodular lesions is the most common parenchymal disease pattern seen in patients with pulmonary sarcoidosis (75%–90% of cases). High-resolution CT shows sharply defined, small (2–4 mm in diameter), rounded nodules, usually with a bilateral and symmetric distribution, predominantly but not invariably in the upper and middle zones. The nodules are found most often in the subpleural peribronchovascular interstitium and less often in the interlobular septa. Although sarcoid granulomas arise as micronodular lesions, they may coalesce over time, forming larger lesions (macronodules) (29,32,38) (Fig 3).

Sarcoid granulomas frequently cause nodular or irregular thickening of the peribronchovascular interstitium. Extensive peribronchovascular

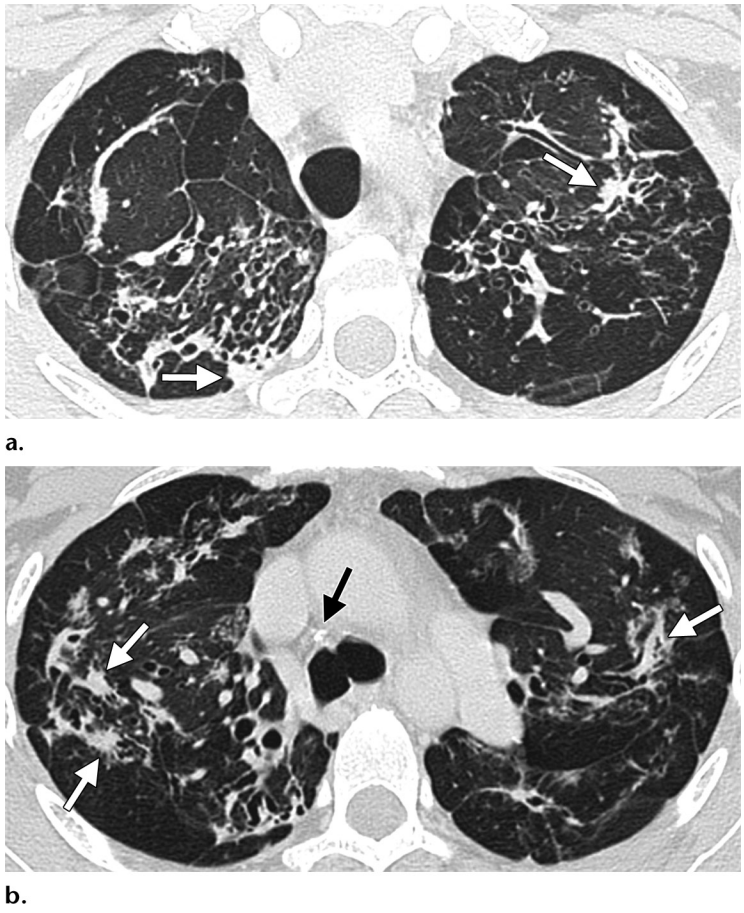

Figure 4. Axial high-resolution CT scans obtained at the level of the upper lobes **(a)** and carina **(b)** in a patient with pulmonary sarcoidosis show a fibrotic-cicatricial pattern of disease, with multiple lesions in a peribronchovascular distribution. Characteristic features of chronic disease are depicted, including traction bronchiectasis, severe architectural distortion, volume loss, and interlobular septal thickening. Coalescent irregular masslike opacities (white arrows) and a calcified right lower paratracheal node (black arrow in **b**) also are seen. Mosaic attenuation, which is most visible in **a**, presumably results from airway distortion due to fibrosis.

nodularity on high-resolution CT images is strongly suggestive of sarcoidosis. However, interstitial thickening is not extensive in most patients with sarcoidosis.

Fibrotic Changes

In most patients, sarcoid granulomas resolve with time. However, in an estimated 20% of patients, fibrosis becomes more prominent over time, producing CT and radiographic findings of linear opacities, traction bronchiectasis, and architectural distortion (displacement of fissures and bronchovascular bundles). Fibrosis is seen predominantly in the upper and middle zones, in a patchy distribution (39) (Fig 4).

Extensive interstitial fibrosis can cause pulmonary arterial hypertension and resultant right heart failure. Imaging findings that may be predictive of such an event include a prominent main pulmonary artery, enlarged right and left pulmonary arteries, right ventricular enlargement, and attenuation of peripheral vessels.

Bilateral Perihilar Opacities

Confluent nodular opacities that appear on high-resolution CT images as bilateral areas of lung consolidation with irregular edges and blurred margins, radiating from the hilum toward the periphery, are often seen with or without air bronchograms. These areas of consolidation are less homogeneous peripherally and are usually accompanied by micronodules (28,30,39) (Fig 5).

Atypical Parenchymal Manifestations

Pulmonary Nodules and Masses

Pulmonary nodules and masses are seen in 15%–25% of patients with parenchymal opacities. At CT, they usually appear as ill-defined irregular opacities measuring 1–4 cm in diameter that represent coalescent interstitial granulomas. These lesions are typically multiple and bilateral, and they may be located in perihilar or peripheral regions (15,28,33). They may or may not manifest with air bronchograms, but they rarely manifest with cavitation (in <3% of patients with parenchymal opacities). Small satellite nodules are often visible at the periphery of these masses, producing an appearance that has been termed the "galaxy sign" (40) (Fig 6). The same sign may be seen also in the presence of other granulomatous diseases and neoplasms.

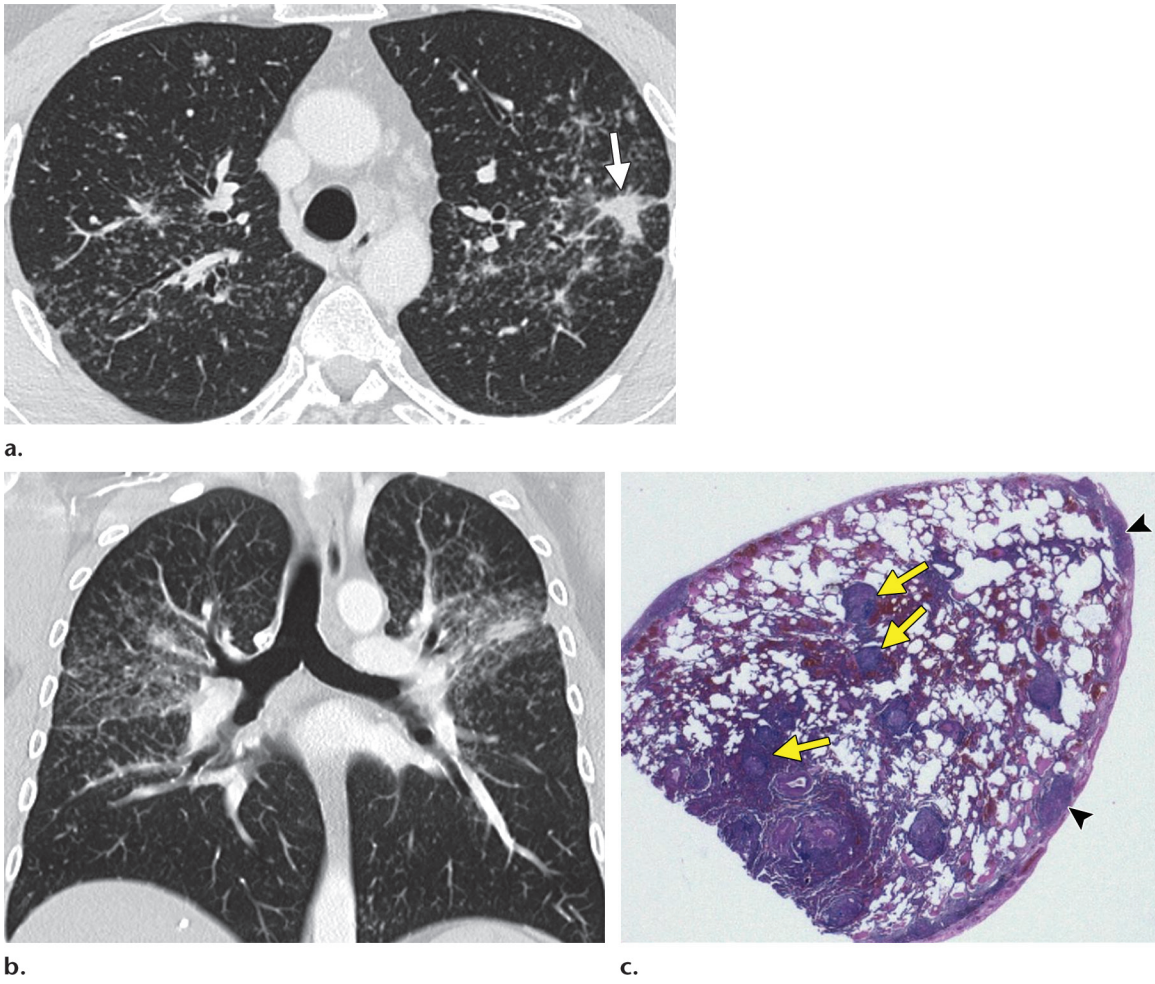

Figure 5. Typical manifestations of pulmonary sarcoidosis. **(a)** Axial high-resolution CT scan shows multiple micronodules with a peribronchovascular distribution in both lungs, predominantly in the upper and middle lobes. One cluster of nodules in the periphery of the left upper lobe (arrow) has coalesced to form a conglomerate lesion (macronodule). **(b)** Coronal reformatted image from high-resolution CT clearly shows upper-lobe predominance of the micronodules. **(c)** Low-magnification photomicrograph (original magnification, ×40; H-E stain) of a coronal slice from the lower part of the right upper lobe shows multiple confluent granulomas infiltrating the peribronchovascular (arrows) and subpleural (arrowheads) interstitium.

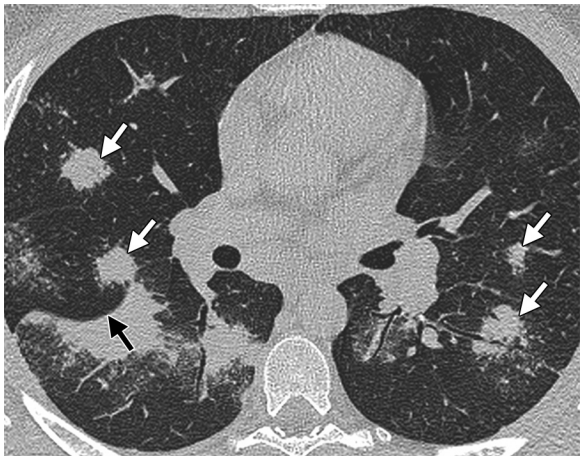

Figure 6. Axial high-resolution CT scan shows several large, ill-defined nodules and areas of consolidation resulting from the confluence of multiple parenchymal micronodules composed of numerous tiny granulomas in both lungs. Fine nodular opacities are seen around the large nodules (white arrows), and small low-attenuation spots that correspond to the spaces between partially coalescent small nodules are visible peripherally. This appearance has been termed the sarcoid galaxy sign. Distortion of the right major fissure is also seen (black arrow).

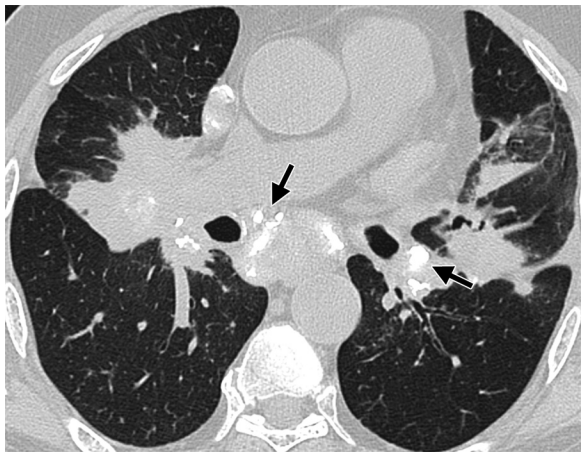

Figure 7. Axial high-resolution CT scan (pulmonary parenchymal window) shows bilateral enlargement and peripheral calcification of mediastinal and hilar lymph nodes (arrows). Calcification also is visible within bilateral hilar parenchymal masses formed by multiple coalescent nodules with a peribronchovascular distribution. Histologic analysis of a specimen obtained at transbronchial biopsy of one of the masses showed sarcoid granulomas. Conglomerate masses and eggshell-like nodal calcifications also may be seen in silicosis, but they are more typically posteriorly situated within the upper lobes, not in hilar locations.

A recently described CT sign, the "sarcoid cluster," consists of multiple micronodules distributed along the lymph vessels on high-resolution CT images (41). This CT feature corresponds to pathologic findings of noncaseous, noncoalescent granulomas with a predominance of CD4-expressing lymphocytes and without fibrosis. Most such micronodule clusters are rounded and are found in deep subpleural locations, in peripheral regions of the upper and middle zones of the lungs.

Occasionally, parenchymal lesions coalesce, forming conglomerate masses that consist of peribronchovascular fibrous tissue surrounding abnormal conglomerations of perihilar bronchi and vessels. These masses, which are typically seen bilaterally in the upper and middle lung zones, may mimic progressive massive fibrosis. Although such lesions are typical of silicosis, they may be observed also in other conditions (eg, berylliosis, tuberculosis, and talcosis), which should be included in the differential diagnosis (29,32,36,38,42) (Fig 7).

A solitary lung mass or nodule is rarely seen in sarcoidosis; however, individual granulomas that coalesce may produce the appearance of solitary masslike opacities (43). In some clinical contexts, multiple well-defined rounded macronodules (nodules with diameters exceeding 5 mm [44]) might mimic a metastatic process (Fig 8).

Patchy Airspace Consolidation

Alveolar or airspace opacification is seen in 10%–20% of patients with sarcoidosis. It is usually bilateral and symmetric and predominantly involves the peribronchovascular regions of the middle and upper zones of the lungs. These central regions of consolidation, which may contain air bronchograms, commonly have ill-defined margins, as consolidation "fades" to a nodular pattern toward the lung periphery. Airspace consolidation in sarcoidosis reflects the confluence of numerous micronodules (acinar and interstitial) that compress the surrounding alveoli or encroach on the alveolar spaces. These coalescent nodules typically appear as multiple radiographic opacities larger than 5 mm in diameter, a pattern referred to as the acinar or alveolar form of sarcoidosis, which may mimic pneumonia, tuberculosis, or bronchiolitis obliterans organizing pneumonia (Fig 9) (37,45).

Patchy Ground-Glass Opacities

Patchy ground-glass opacities are seen in an estimated 40% of patients with parenchymal changes due to pulmonary sarcoidosis; extensive ground-glass opacities are much less common. The patchy ground-glass opacities in sarcoidosis result from the confluence of multiple micronodular granulomatous and fibrotic interstitial lesions, which cause airway compression but not airspace filling like that seen in alveolitis (9,33). These ground-glass opacities have ill-defined margins,

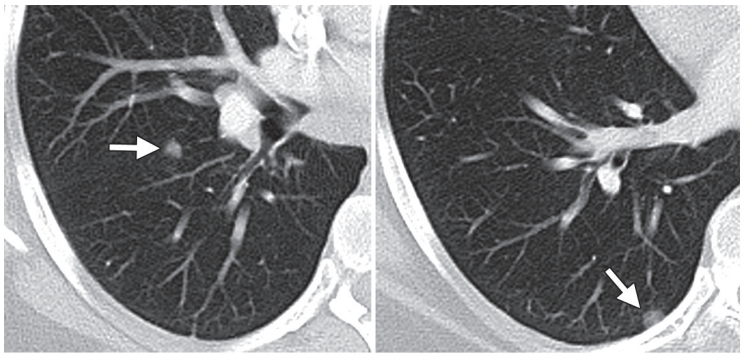

a.

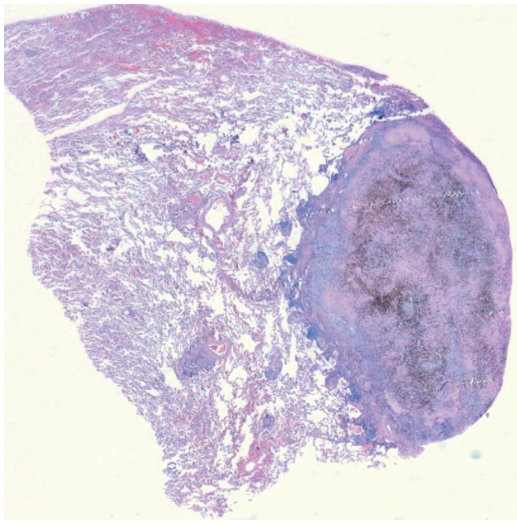

b.

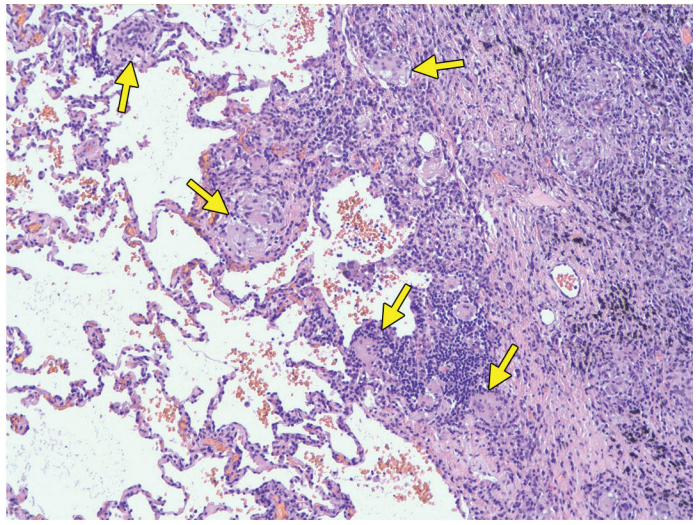

c.

Figure 8. Sarcoidosis in a patient with a history of stage III primary cutaneous malignant melanoma. **(a)** Contrast-enhanced CT scans show pulmonary nodules (arrow) in subpleural (right) and fissural (left) regions. A video-assisted thoracoscopic surgical biopsy was performed. **(b)** Low-power photomicrograph (original magnification, ×10; H-E stain) obtained at histopathologic analysis shows a subpleural nodule that is darker in color because of anthracosis. **(c)** Photomicrograph obtained at higher power (original magnification, ×100; H-E stain) shows multiple nonnecrotic granulomas (arrows) expanding the interstitium that surrounds the subpleural nodule in **b**.

Figure 9. Alveolar sarcoid pattern of airspace consolidation in pulmonary sarcoidosis. Axial high-resolution CT scan shows alveolar consolidation in the left upper lobe and patchy subpleural alveolar opacities in the right upper lobe. Architectural distortion and traction bronchiectasis, signs of fibrosis, also are visible, mainly in the right upper lobe.

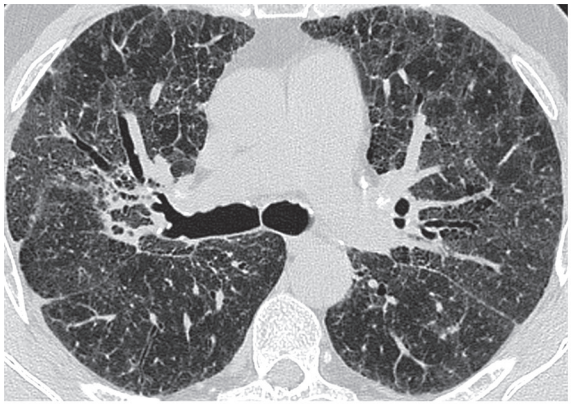

10.

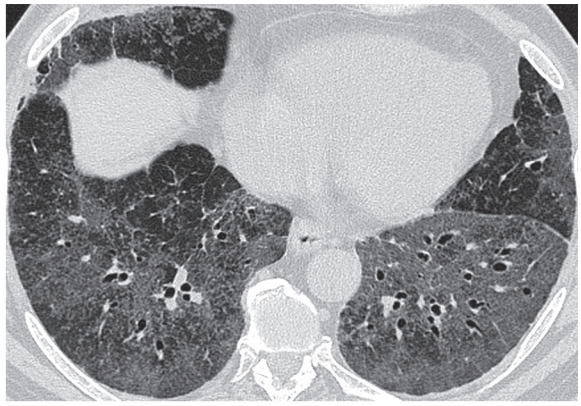

11a.

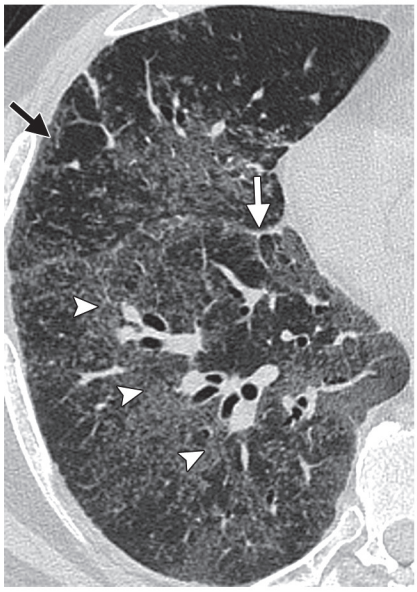

11b.

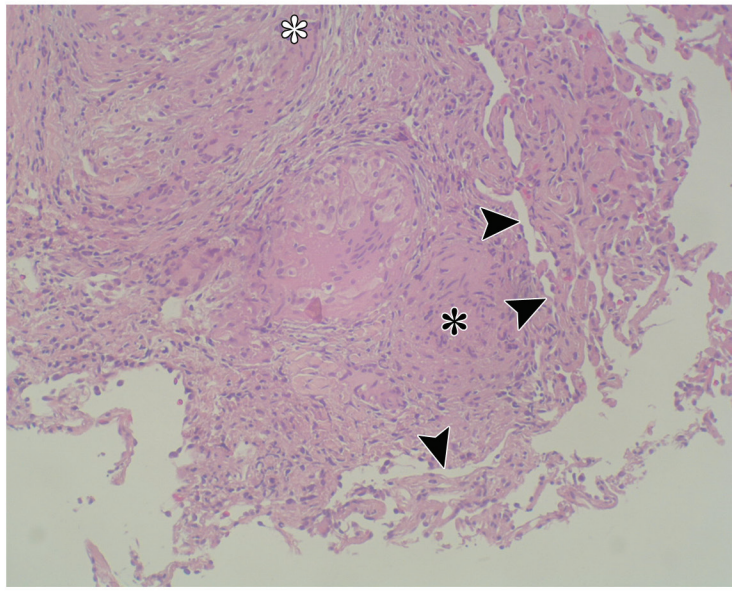

11c.

Figures 10, 11. Ground-glass opacities in pulmonary sarcoidosis. **(10)** Axial high-resolution CT scan obtained at the level of the carina depicts patchy ground-glass opacities resulting from multiple coalescent micronodules in a peribronchovascular and subpleural distribution. Other changes depicted, all of which are indicative of fibrosis, include traction bronchiectasis, architectural distortion, cystic lesions, and septal thickening. **(11a)** Axial high-resolution CT scan shows a diffuse ground-glass pattern produced by multiple confluent micronodules, with associated bronchiectasis. **(11b)** Magnified axial high-resolution CT scan of the right lung clearly depicts separate nodules in a subpleural (black arrow) and fissural (white arrow) distribution and along the bronchovascular bundles (arrowheads). **(11c)** High-power photomicrograph (original magnification, ×250; H-E stain) of a specimen obtained at wedge biopsy shows an accumulation of interstitial granulomas (white ∗), which causes a thickened appearance of the interalveolar septa, and acinar granulomas (black ∗), which form in the interstitium of the alveolar wall and protrude into the alveoli (arrowheads).

and bronchoalveolar structures are frequently visible within them at CT. Occasionally, intraalveolar granulomas, scattered desquamative cells, or hyaline membranes may lead to airspace opacity; however, the airways are more often patent, producing the appearance of air bronchograms at CT (Figs 10, 11).

The patchy ground-glass opacities in sarcoidosis are always accompanied by other abnormalities and often are superimposed on a background of interstitial nodules. However, the same pattern can be seen in bronchoalveolar cell carcinoma,

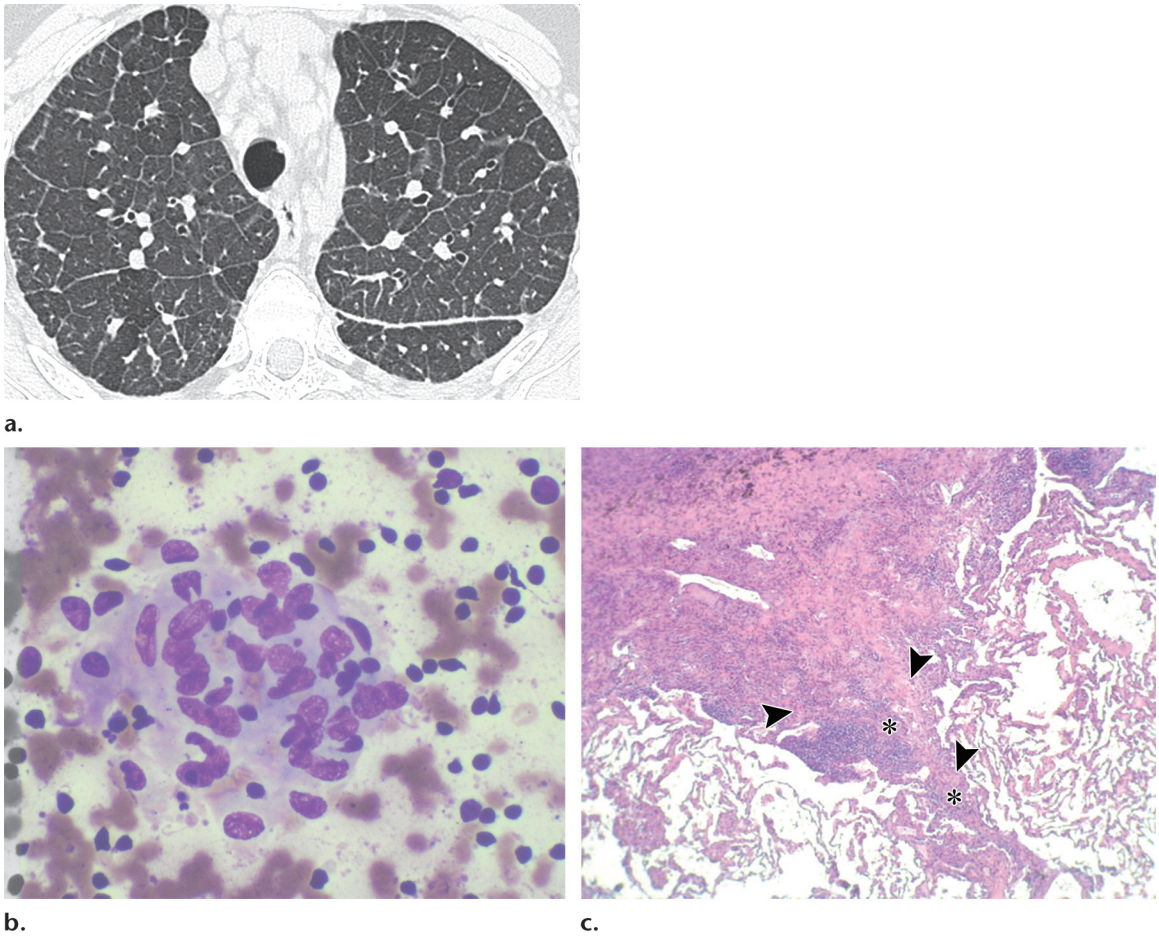

Figure 12. **(a)** Axial high-resolution CT scan shows mediastinal lymph node enlargement and a reticular pattern produced by nodularity and thickening of interlobular septa, pleural surfaces, and fissures, features that are seen in lymphangitic carcinomatosis as well as sarcoidosis. **(b)** Photomicrograph (original magnification, ×400; Giemsa stain) of a specimen from fine-needle aspiration biopsy of an enlarged right paratracheal lymph node shows a group of histiocytes against a lymphocytic background, a cytologic structure characteristic of sarcoid granuloma. **(c)** Photomicrograph (original magnification, ×100; H-E stain) of a lung biopsy specimen from another patient shows progressive thickening of the interlobular septum (*) because of the accumulation of numerous sarcoid granulomas (arrowheads), an appearance that correlates well with the CT features seen in **a**.

lymphoma, pneumoconiosis, pneumonia, and bronchiolitis obliterans organizing pneumonia.

Linear Reticular Opacities

Isolated linear reticular opacities are observed in an estimated 50% of patients with sarcoidosis, but a linear pattern is the predominant radiologic feature of the disease in only 15%–20% of patients. This pattern is produced by interlobular and intralobular septal thickening and usually is seen in the subpleural space in the upper and middle lung zones (15,28–30). Interlobular septal thickening that is marked and irregular may simulate lymphangitic carcinomatosis. However, lymphangitic carcinomatosis is characterized by more extensive and more severe involvement of the interlobular septa and subpleural space on high-resolution CT images than is typical either in lymphoma or in sarcoidosis (46) (Fig 12).

Fibrocystic Changes

Fibrotic cysts, bullae, and paracicatricial emphysema represent advanced-stage sarcoidosis. Fibrotic and cystic lesions typically involve the upper and middle lung zones and follow the large airways in a perihilar distribution.

Figure 13. Axial unenhanced high-resolution CT scan obtained in a patient with stage 4 sarcoidosis shows bilateral cystic spaces and cavities (arrow) and tracheal retraction, results of chronic severe fibrosis and scarring. The cystic spaces in the left perihilar region (*) correspond to dilated bronchi. The fibrotic-cystic lesions that occur in sarcoidosis typically involve the upper and middle lung zones and follow the large airways in a perihilar distribution.

Posterior displacement of the main or upper-lobe bronchus and volume loss (particularly in the upper lobes) are characteristic features of chronic fibrosis (Fig 13).

Honeycomb-like Cysts.—Honeycomb-like cysts in patients with sarcoidosis are most commonly distributed in the subpleural regions of the middle and upper lung zones, whereas the lung bases are usually spared (39). Occasionally this pattern of fibrocystic change is seen in the lower lung zones, an atypical location that may cause pulmonary sarcoidosis to be mistaken for idiopathic pulmonary fibrosis (Fig 14).

Cavitation of Parenchymal Lesions.—Cavitation of parenchymal lesions is a rare finding in sarcoidosis. It is seen in an estimated 10% of patients with end-stage disease (36). Primary cavitary sarcoidosis, with central necrosis due to confluent granulomas lining the walls of a pulmonary cavity, is rare (<0.8% of cases of sarcoidosis) (47) and usually occurs in young individuals with acinar or nodular disease (48). Most apparent cavities seen on chest radiographs and CT images are in fact bullae, blebs, or cysts that developed in the advanced fibrocystic stage of sarcoidosis (49). These pseudocavities are lined by dense fibrous tissue, not by granulomas, because cavitation most often occurs in areas of advanced fibrosis.

Mycetoma Formation.—The formation of mycetomas is a well-recognized complication of stage 4 cystic sarcoidosis. Fungal balls may develop when preexisting bullae and cysts (typically in the upper lobes) are colonized by saprophytic fungi, usually *Aspergillus* species. When cavities are secondarily infected, they may resemble the thick-walled cavities seen in pyogenic lung abscesses. Air-fluid levels within sarcoid pseudocavities are one of the first signs of superimposed fungal infection. The characteristic radiographic appearance of pulmonary aspergillomas consists of a mobile opacity occupying part or most of the cavity and bordered by a peripheral sliver of air known as the air crescent or Monod sign (50) (Fig 15). New pleural thickening adjacent to a known cystic space usually precedes the fungus ball or air crescent sign. The frequency of occurrence of aspergilloma as a complication of pulmonary sarcoidosis ranges from 1% to 3% of cases but is higher in the subset of cases of radiographic stage 3 or 4 sarcoidosis (51).

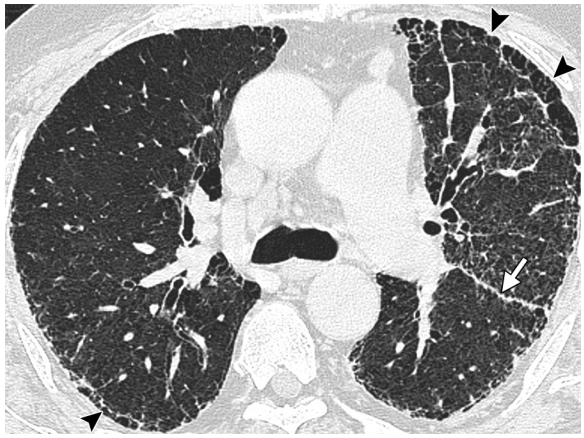

Figure 14. Axial unenhanced high-resolution CT scan shows asymmetric subpleural honeycomb-like cysts (arrowheads) and architectural distortion associated with left fissure nodularity (arrow). Although these features also are characteristic of idiopathic pulmonary fibrosis, the upper-lobe predominance of honeycomb-like cysts and the peribronchovascular and fissural distribution of micronodules in this case were more suggestive of sarcoidosis.

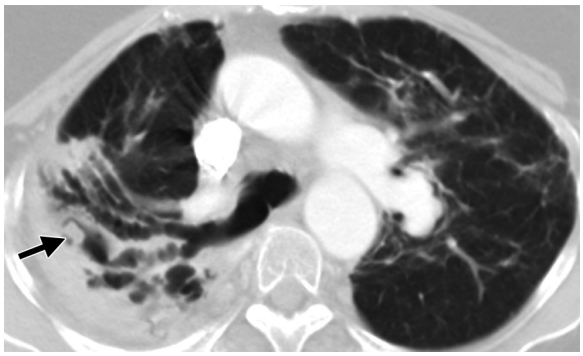

Figure 15. Axial contrast-enhanced CT scan obtained in a patient with stage 4 sarcoidosis depicts a mycetoma (aspergilloma) within a cystic space in the right upper lobe. The opaque fungal ball is bordered on one side by the air crescent or Monod sign (arrow). Retraction of the trachea and right upper lobe bronchus, caused by severe fibrosis and scarring, also are depicted.

Figure 16. Miliary opacities in sarcoidosis. Axial unenhanced high-resolution CT scan shows countless tiny micronodules representing multiple and diffuse granulomas in a random distribution, with bronchial wall thickening. When this pattern is seen, the differential diagnosis should include miliary tuberculosis, pneumoconiosis, and metastatic lesions.

Aspergillomas are associated with hemoptysis, a common symptom that is occasionally massive and life threatening. This type of pulmonary hemorrhage is the second most common cause of death among patients with sarcoidosis (52). The walls of aspergillomas are supplied by branches of the bronchial arteries, which tend to bleed easily into the cavity. Various hypotheses have been proffered to explain why aspergillomas cause hemorrhage, including invasion of blood vessels in the cavity wall by *Aspergillus*, the effect of endotoxins produced by *Aspergillus*, and mechanical friction from the fungal ball (53). There is also evidence that the presence of the aspergilloma may induce an inflammatory reaction, causing locally elevated blood levels of vascular endothelial growth factor that promote angiogenesis in the cavity wall (54). The neovessels produced by this process have fragile walls and tend to bleed easily into the cavity.

Miliary Opacities

This pattern is rare in sarcoidosis (<1% of cases), and its appearance at imaging may warrant the inclusion of entities such as tuberculosis, pneumoconiosis, and metastatic lesions in the differential diagnosis (Fig 16). Histoplasmosis, chickenpox, and Langerhans cell histiocytosis are other entities that might also be included in the differential diagnosis; however, miliary opacities are manifested even more rarely in these conditions than in sarcoidosis (55).

Airway Involvement

The most common manifestations of airway involvement at high-resolution CT in patients with sarcoidosis are a mosaic attenuation pattern, air trapping, tracheobronchial abnormalities, and atelectasis.

Mosaic Attenuation Pattern.—Mosaic attenuation refers to inhomogeneous attenuation seen at inspiratory CT. This pattern may represent patchy interstitial disease, small airways disease, or vascular disease. In patients with sarcoidosis, mosaic attenuation most often results from small airways involvement by granulomas or fibrosis, which may lead to obstruction (56,57). To verify that the CT finding is caused by air trapping, a finding of mosaic attenuation on inspiratory images must be compared with the parenchymal appearance on expiratory images (Fig 17).

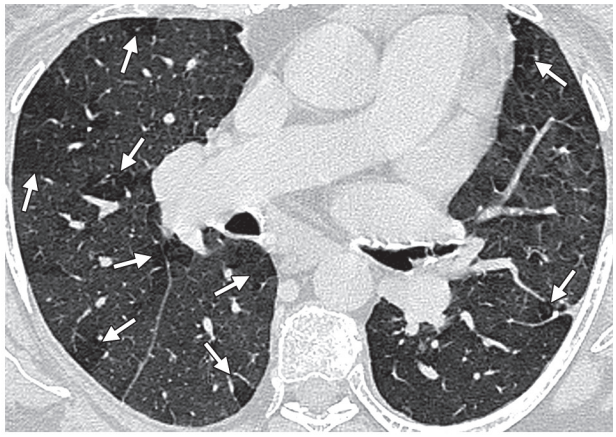

a.

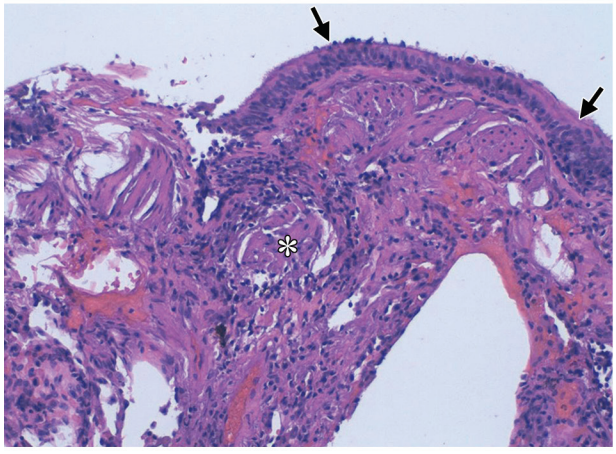

b.

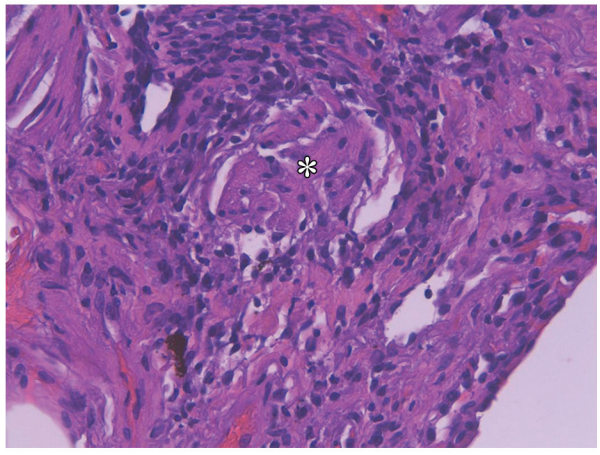

c.

Figure 17. **(a)** Axial unenhanced high-resolution expiratory CT scan obtained in a patient with pulmonary sarcoidosis shows a mosaic pattern consisting of multiple areas of low attenuation (arrows) interspersed with larger areas of normal lung parenchyma. This appearance is produced by air trapping. **(b, c)** Photomicrographs (original magnification of **b**, ×100; original magnification of **c**, ×250; H-E stain) of a transbronchial lung biopsy specimen show accumulations of sarcoid granulomas (*) in the mucosal and submucosal layers of bronchiolar epithelium (arrows in **b**).

Air Trapping.—Multiple studies have shown that air trapping is a common, albeit nonspecific, feature of pulmonary sarcoidosis (95% of patients) (56,58). There is no difference between the radiographic stages of disease (stages 1–4) with regard to the prevalence or extent of air trapping characterized by focal areas of decreased attenuation on expiratory CT images (56–58) (Fig 17). Thus, many different factors likely contribute to air trapping in pulmonary sarcoidosis. Although expiratory CT images obtained in most patients with pulmonary sarcoidosis show air trapping in locations suggestive of small airways disease, some studies have demonstrated that air trapping may occur at the level of the secondary lobule, as well as in distributions suggestive of sublobular, subsegmental, and segmental involvement (58,59).

Tracheobronchial Abnormalities.—Bronchial stenosis due to large airways disease is a relatively common incidental finding at bronchoscopy in patients with pulmonary sarcoidosis. In contrast, symptomatic bronchial stenosis is rare; it is believed to occur in only 2%–8% of patients (34). Stenosis or compression of bronchi may result from accumulation of endobronchial granulomas within the bronchial wall, extrinsic compression of the large airways by enlarged hilar nodes, or distortion of major bronchi by end-stage parenchymal disease (60). Stenosis, irregularity, distortion, clustering, and focal areas of bronchiectasis have been reported in studies performed with bronchography (60) and CT (34) in patients with sarcoidosis. The right middle lobe bronchus is particularly vulnerable to obstruction because of its length, its relatively small caliber, the acute angle of its origin from the bronchus intermedius, and its proximity to lymph nodes that drain the right lower lobe as well as the middle and upper lobes (61) (Fig 18).

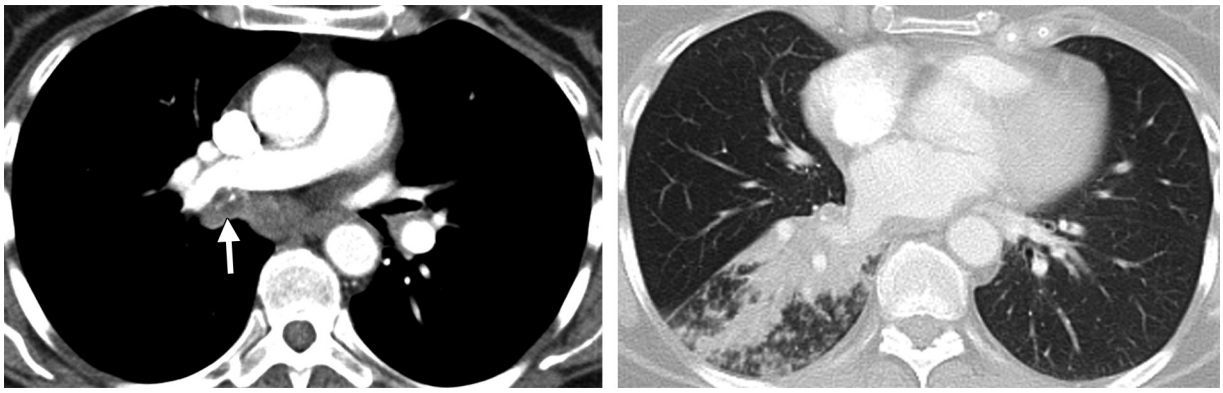

a. b.

Figure 18. Tracheobronchial and pulmonary involvement of sarcoidosis in a patient with hemoptysis after repeated surgical interventions for tracheal stenosis. **(a)** Axial contrast-enhanced CT scan obtained at the subcarinal level shows a soft-tissue mass with punctate calcifications that fills the lumen of the right intermediate bronchus (arrow), causing partial atelectasis of the right middle and right lower lobes. Mild bilateral hilar lymphadenopathy and marked subcarinal lymphadenopathy also are seen. **(b)** Axial contrast-enhanced CT scan (parenchymal window) obtained at the level of basal segmental lower lobe bronchi shows that part of the mass encases and occupies the right lower lobe bronchi, causing partial atelectasis. At diagnostic thoracotomy, sarcoidosis with tracheobronchial and pulmonary involvement was found.

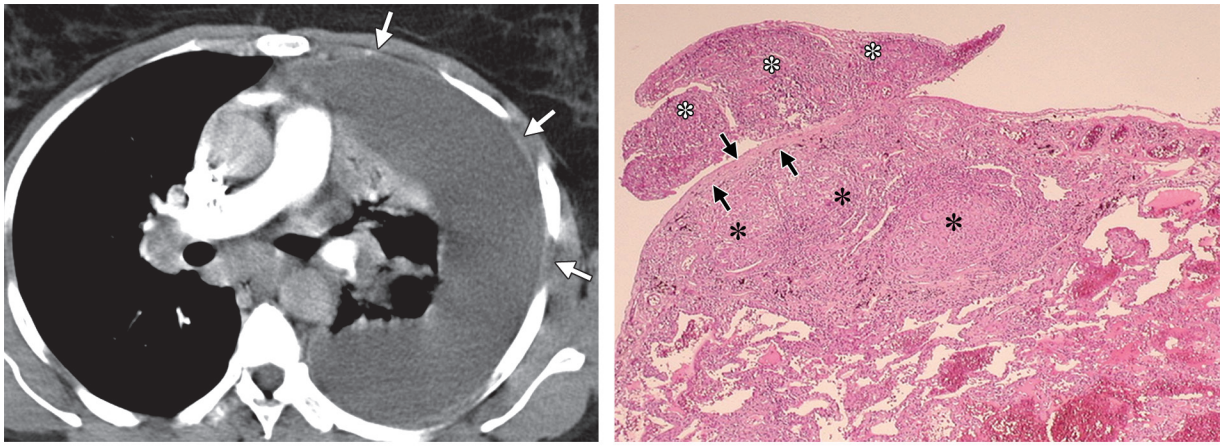

a. b.

Figure 19. **(a)** Axial contrast-enhanced CT scan obtained at the subcarinal level in a patient with pulmonary sarcoidosis shows chronic pleural effusion, diffuse pleural thickening (arrows), and hilar and mediastinal lymphadenopathy. **(b)** Photomicrograph (original magnification, ×100; H-E stain) of a thoracoscopic lung biopsy specimen shows conglomerations of sarcoid granulomas underlying (black ∗) and protruding outward (white ∗) from the pleural surface (arrows).

Atelectasis.—The obstruction of lobar or segmental bronchi by small endobronchial granulomas or enlarged peribronchial lymph nodes results in atelectasis (34,60) (Fig 18).

Pleural Disease

Pleural involvement in sarcoidosis is rare, occurring in only 1%–4% of patients (62). Manifestations of pleural involvement include exudative or transudative pleural effusion, hemorrhagic or chylous pleural effusion (chylothorax being an exceptionally rare complication caused by involvement of the mediastinal lymph nodes or the thoracic duct [63]), pneumothorax, pleural thickening, and, rarely, pleural calcification. Pleural effusions are usually minimal and resolve within 2–3 months, although massive effusions have been reported (Fig 19). Pneumothorax, a sequela of advanced bullous disease seen in the

late fibrotic stages of sarcoidosis, may result from rupture of an emphysematous bleb or necrosis of a subpleural sarcoid granuloma (62).

Pleural Plaquelike Opacities

Pleural plaquelike opacities are pulmonary opacities that simulate pleural plaques. Formed by multiple coalescent micronodules (granulomas), these lesions usually have well-defined irregular margins. They are seen bilaterally in regions contiguous with the pleura, mostly in the upper and middle lung zones, sometimes with associated pleural effusion. Pleural plaquelike opacities are most commonly found in sarcoidosis, silicosis, and coal-worker's pneumoconiosis (64).

Conclusions

Thoracic sarcoidosis has been called "the great mimic"; it manifests with various patterns at radiologic imaging, necessitating an initially broad differential diagnosis that includes lymphoma, tuberculosis, and many other causes of chronic pulmonary infiltrates. Severe thoracic sarcoidosis causes significant clinical and functional impairment and is associated with high morbidity and mortality.

In most patients with sarcoidosis, pulmonary abnormalities are seen during imaging at some stage of the disease. In 60%–70% of patients, the characteristic feature is enlarged hilar and paratracheal lymph nodes, with or without concomitant parenchymal changes (3). However, the imaging findings are nonspecific or atypical in 25%–30% of patients, and in another 5%–10%, no abnormalities are seen at thoracic imaging (3,32).

CT has proved superior to radiography for identifying and managing pulmonary sarcoidosis. High-resolution CT helps improve the detection and characterization of subtle parenchymal abnormalities beyond the levels achievable with radiography and conventional CT, contributing to increased diagnostic accuracy (65,66). High-resolution CT is capable of providing significant anatomic information about interstitial lung disease. It is particularly helpful for differentiating active inflammation from fibrosis in patients with stage 2 or 3 sarcoidosis (28–30).

Radiologists can play an essential role in the diagnosis and management of sarcoidosis. It is essential to recognize both the typical and the atypical manifestations of the disease, take note of those that also may occur in diseases other than sarcoidosis, and use information obtained from the correlation of imaging features with pathologic findings to help achieve an early diagnosis and reduce associated morbidity and mortality.

References

1. Statement on sarcoidosis. Joint Statement of the American Thoracic Society (ATS), the European Respiratory Society (ERS) and the World Association of Sarcoidosis and Other Granulomatous Disorders (WASOG) adopted by the ATS Board of Directors and by the ERS Executive Committee, February 1999. Am J Respir Crit Care Med 1999;160(2):736–755.
2. Rybicki BA, Iannuzzi MC, Frederick MM, et al. Familial aggregation of sarcoidosis: a case-control etiologic study of sarcoidosis (ACCESS). Am J Respir Crit Care Med 2001;164(11):2085–2091.
3. Hillerdal G, Nöu E, Osterman K, Schmekel B. Sarcoidosis: epidemiology and prognosis—a 15-year European study. Am Rev Respir Dis 1984;130(1):29–32.
4. Henke CE, Henke G, Elveback LR, Beard CM, Ballard DJ, Kurland LT. The epidemiology of sarcoidosis in Rochester, Minnesota: a population-based study of incidence and survival. Am J Epidemiol 1986;123(5):840–845.
5. James DG, Hosoda Y. Epidemiology. In: James DG, ed. Sarcoidosis and other granulomatous disorders. New York, NY: Dekker, 1994; 729–744.
6. Xaubet A, Ancochea J, Morell F, et al. Report on the incidence of interstitial lung diseases in Spain. Sarcoidosis Vasc Diffuse Lung Dis 2004;21(1):64–70.
7. Siltzbach LE, James DG, Neville E, et al. Course and prognosis of sarcoidosis around the world. Am J Med 1974;57(6):847–852.
8. Reich JM. Mortality of intrathoracic sarcoidosis in referral vs population-based settings: influence of stage, ethnicity, and corticosteroid therapy. Chest 2002;121(1):32–39.
9. Lynch JP 3rd, Kazerooni EA, Gay SE. Pulmonary sarcoidosis. Clin Chest Med 1997;18(4):755–785.
10. Baughman RP, Teirstein AS, Judson MA, et al. Clinical characteristics of patients in a case control study of sarcoidosis. Am J Respir Crit Care Med 2001;164(10 pt 1):1885–1889.
11. Lynch JP 3rd, White ES. Pulmonary sarcoidosis. Eur Respir Monogr 2005;10:105–129.
12. Cieslicki J, Zych D, Zielinski J. Airways obstruction in patients with sarcoidosis. Sarcoidosis 1991;8(1):42–44.
13. Handa T, Nagai S, Fushimi Y, et al. Clinical and radiographic indices associated with airflow limitation in patients with sarcoidosis. Chest 2006;130(6):1851–1856.

14. Neville E, Walker AN, James DG. Prognostic factors predicting the outcome of sarcoidosis: an analysis of 818 patients. Q J Med 1983;52(208):525–533.
15. Brauner MW, Lenoir S, Grenier P, Cluzel P, Battesti JP, Valeyre D. Pulmonary sarcoidosis: CT assessment of lesion reversibility. Radiology 1992;182(2):349–354.
16. Baughman RP, Winget DB, Bowen EH, Lower EE. Predicting respiratory failure in sarcoidosis patients. Sarcoidosis Vasc Diffuse Lung Dis 1997;14(2):154–158.
17. Miller BH, Rosado-de-Christenson ML, McAdams HP, Fishback NF. Thoracic sarcoidosis: radiologic-pathologic correlation. RadioGraphics 1995;15(2):421–437.
18. Newman LS, Rose CS, Maier LA. Sarcoidosis. N Engl J Med 1997;336(17):1224–1234.
19. Rosen Y. Sarcoidosis. In: Dail DH, Hammer SP, eds. Pulmonary pathology. New York, NY: Springer-Verlag, 1994; 13–645.
20. Churg A, Carrington CB, Gupta R. Necrotizing sarcoid granulomatosis. Chest 1979;76(4):406–413.
21. Takemura T, Matsui Y, Saiki S, Mikami R. Pulmonary vascular involvement in sarcoidosis: a report of 40 autopsy cases. Hum Pathol 1992;23(11):1216–1223.
22. Siltzbach LE. Sarcoidosis: clinical features and management. Med Clin North Am 1967;51(2):483–502.
23. Hunsaker AR, Munden RF, Pugatch RD, Mentzer SJ. Sarcoidlike reaction in patients with malignancy. Radiology 1996;200(1):255–261.
24. Trisolini R, Lazzari Agli L, Cancellieri A, et al. Transbronchial needle aspiration improves the diagnostic yield of bronchoscopy in sarcoidosis. Sarcoidosis Vasc Diffuse Lung Dis 2004;21(2):147–151.
25. Zwischenberger JB, Savage C, Alpard SK, Anderson CM, Marroquin S, Goodacre BW. Mediastinal transthoracic needle and core lymph node biopsy: should it replace mediastinoscopy? Chest 2002;121(4):1165–1170.
26. Silvestri GA. The mounting evidence for endobronchial ultrasound. Chest 2009;136(2):327–328.
27. Garwood S, Judson MA, Silvestri G, Hoda R, Fraig M, Doelken P. Endobronchial ultrasound for the diagnosis of pulmonary sarcoidosis. Chest 2007;132(4):1298–1304.
28. Brauner MW, Grenier P, Mompoint D, Lenoir S, de Crémoux H. Pulmonary sarcoidosis: evaluation with high-resolution CT. Radiology 1989;172(2):467–471.
29. Müller NL, Kullnig P, Miller RR. The CT findings of pulmonary sarcoidosis: analysis of 25 patients. AJR Am J Roentgenol 1989;152(6):1179–1182.
30. Nishimura K, Itoh H, Kitaichi M, Nagai S, Izumi T. CT and pathological correlation of pulmonary sarcoidosis. Semin Ultrasound CT MR 1995;16(5):361–370.
31. Müller NL, Miller RR. Ground-glass attenuation, nodules, alveolitis, and sarcoid granulomas. Radiology 1993;189(1):31–32.
32. Hamper UM, Fishman EK, Khouri NF, Johns CJ, Wang KP, Siegelman SS. Typical and atypical CT manifestations of pulmonary sarcoidosis. J Comput Assist Tomogr 1986;10(6):928–936.
33. Nishimura K, Itoh H, Kitaichi M, Nagai S, Izumi T. Pulmonary sarcoidosis: correlation of CT and histopathologic findings. Radiology 1993;189(1):105–109.
34. Lenique F, Brauner MW, Grenier P, Battesti JP, Loiseau A, Valeyre D. CT assessment of bronchi in sarcoidosis: endoscopic and pathologic correlations. Radiology 1995;194(2):419–423.
35. Winterbauer RH, Belic N, Moores KD. Clinical interpretation of bilateral hilar adenopathy. Ann Intern Med 1973;78(1):65–71.
36. Rockoff SD, Rohatgi PK. Unusual manifestations of thoracic sarcoidosis. AJR Am J Roentgenol 1985;144(3):513–528.
37. Conant EF, Glickstein MF, Mahar P, Miller WT. Pulmonary sarcoidosis in the older patient: conventional radiographic features. Radiology 1988;169(2):315–319.
38. Koyama T, Ueda H, Togashi K, Umeoka S, Kataoka M, Nagai S. Radiologic manifestations of sarcoidosis in various organs. RadioGraphics 2004;24(1):87–104.
39. Abehsera M, Valeyre D, Grenier P, Jaillet H, Battesti JP, Brauner MW. Sarcoidosis with pulmonary fibrosis: CT patterns and correlation with pulmonary function. AJR Am J Roentgenol 2000;174(6):1751–1757.
40. Nakatsu M, Hatabu H, Morikawa K, et al. Large coalescent parenchymal nodules in pulmonary sarcoidosis: "sarcoid galaxy" sign. AJR Am J Roentgenol 2002;178(6):1389–1393.
41. Herráez Ortega I, Alonso Orcajo N, López González L. The "sarcoid cluster sign": a new sign in high resolution chest CT [in Spanish]. Radiologia 2009;51(5):495–499.
42. Webb WR, Müller NI, Naidich DP, eds. High resolution CT of the lung. New York, NY: Raven, 1992;76–87.
43. Gotway MB, Tchao NK, Leung JW, Hanks DK, Thomas AN. Sarcoidosis presenting as an enlarging solitary pulmonary nodule. J Thorac Imaging 2001;16(2):117–122.
44. Hansell DM, Bankier AA, MacMahon H, McLoud TC, Müller NL, Remy J. Fleischner Society: glossary of terms for thoracic imaging. Radiology 2008;246(3):697–722.
45. Freundlich IM, Libshitz HI, Glassman LM, Israel HL. Sarcoidosis. Typical and atypical thoracic manifestations and complications. Clin Radiol 1970;21(4):376–383.
46. Honda O, Johkoh T, Ichikado K, et al. Comparison of high resolution CT findings of sarcoidosis, lymphoma, and lymphangitic carcinoma: is there any difference of involved interstitium? J Comput Assist Tomogr 1999;23(3):374–379.
47. Mayock RL, Bertrand P, Morrison CE, Scott JH. Manifestations of sarcoidosis: analysis of 145 patients, with a review of nine series selected from the literature. Am J Med 1963;35:67–89.

48. Rohatgi PK, Schwab LE. Primary acute pulmonary cavitation in sarcoidosis. AJR Am J Roentgenol 1980; 134(6):1199–1203.
49. Ichikawa Y, Fujimoto K, Shiraishi T, Oizumi K. Primary cavitary sarcoidosis: high-resolution CT findings. AJR Am J Roentgenol 1994;163(3):745.
50. Pesle GD, Monod O. Bronchiectasis due to asperigilloma. Dis Chest 1954;25(2):172–183.
51. Wollschlager C, Khan F. Aspergillomas complicating sarcoidosis: a prospective study in 100 patients. Chest 1984;86(4):585–588.
52. Israel HL, Lenchner GS, Atkinson GW. Sarcoidosis and aspergilloma: the role of surgery. Chest 1982; 82(4):430–432.
53. Soubani AO, Chandrasekar PH. The clinical spectrum of pulmonary aspergillosis. Chest 2002;121 (6):1988–1999.
54. Inoue K, Matsuyama W, Hashiguchi T, et al. Expression of vascular endothelial growth factor in pulmonary aspergilloma. Intern Med 2001;40(12): 1195–1199.
55. Wells A. High resolution computed tomography in sarcoidosis: a clinical perspective. Sarcoidosis Vasc Diffuse Lung Dis 1998;15(2):140–146.
56. Davies CW, Tasker AD, Padley SP, Davies RJ, Gleeson FV. Air trapping in sarcoidosis on computed tomography: correlation with lung function. Clin Radiol 2000;55(3):217–221.
57. Hansell DM, Milne DG, Wilsher ML, Wells AU. Pulmonary sarcoidosis: morphologic associations of airflow obstruction at thin-section CT. Radiology 1998;209(3):697–704.
58. Bartz RR, Stern EJ. Airways obstruction in patients with sarcoidosis: expiratory CT scan findings. J Thorac Imaging 2000;15(4):285–289.
59. Stern EJ, Swensen SJ. High-resolution CT of the chest: comprehensive atlas. Philadelphia, Pa: Lippincott-Raven, 1996; 245.
60. Udwadia ZF, Pilling JR, Jenkins PF, Harrison BD. Bronchoscopic and bronchographic findings in 12 patients with sarcoidosis and severe or progressive airways obstruction. Thorax 1990;45(4):272–275.
61. Arkless HA, Chodoff RJ. Middle lobe syndrome due to sarcoidosis. Dis Chest 1956;30(3):351–353.
62. Soskel NT, Sharma OP. Pleural involvement in sarcoidosis: case presentation and detailed review of the literature. Semin Respir Med 1992;13(6): 492–514.
63. Jarman PR, Whyte MK, Sabroe I, Hughes JM. Sarcoidosis presenting with chylothorax. Thorax 1995;50(12):1324–1325.
64. Remy-Jardin M, Beuscart R, Sault MC, Marquette CH, Remy J. Subpleural micronodules in diffuse infiltrative lung diseases: evaluation with thin-section CT scans. Radiology 1990;177(1):133–139.
65. Remy-Jardin M, Remy J, Deffontaines C, Duhamel A. Assessment of diffuse infiltrative lung disease: comparison of conventional CT and high-resolution CT. Radiology 1991;181(1):157–162.
66. Mayo JR, Webb WR, Gould R, et al. High-resolution CT of the lungs: an optimal approach. Radiology 1987;163(2):507–510.

RadioGraphics

Pulmonary Sarcoidosis: Typical and Atypical Manifestations at High-Resolution CT with Pathologic Correlation

Eva Criado, MD • Marcelo Sánchez, MD • José Ramírez, MD, PhD • Pedro Arguis, MD • Teresa M. de Caralt, MD, PhD • Rosario J. Perea, MD, PhD • Antonio Xaubet, MD, PhD

RadioGraphics 2010; 30:1567–1586 • **Published online** 10.1148/rg.306105512 • **Content Codes:** CH CT

Page 1568
Involvement of the lung and the mediastinal and hilar lymph nodes is most common, being seen in approximately 90% of patients, and accounts for most of the morbidity and mortality associated with the condition (1).

Page 1569
Granulomas in the lung parenchyma have a characteristic distribution in relation to lymphatics in the peribronchovascular interstitial space, subpleural interstitial space, and, to a lesser extent, the interlobular septa (ie, a lymphangitic distribution).

Page 1569
More than 40 years ago, Siltzbach developed a sarcoidosis staging system based on the pattern of chest radiographic findings, a system still widely used because of its great prognostic value (22).

Page 1571 (Table on page 1571)
High-resolution CT may be particularly helpful for distinguishing active inflammation from irreversible fibrosis in selected patients with stage 2 or 3 sarcoidosis. Nodules, ground-glass opacities, and alveolar opacities are suggestive of granulomatous inflammation that may be reversed with therapy (31). By contrast, honeycomb-like cysts, bullae, broad and coarse septal bands, architectural distortion, volume loss, and traction bronchiectasis are indicative of irreversible fibrosis (16) (Table 2).

Page 1572
The most common pattern is well-defined, bilateral, symmetric hilar and right paratracheal lymph node enlargement. Bilateral hilar lymph node enlargement, alone or in combination with mediastinal lymph node enlargement, occurs in an estimated 95% of patients affected with sarcoidosis (4,8,9).